Novel analyses of long-term data provide a scientific basis for chlorophyll-a thresholds in San Francisco Bay

Martha Sutula [a, *], Raphael Kudela [b], James D. Hagy III [c], Lawrence W. Harding Jr. [d], David Senn [e], James E. Cloern [f], Suzanne Bricker [g], Gry Mine Berg [h], Marcus Beck [c]

[a] Southern California Coastal Water Research Project, Costa Mesa, CA 92626, USA
[b] Ocean Sciences Department, University of California Santa Cruz, CA 95064, USA
[c] U.S. Environmental Protection Agency, Office of Research and Development, Gulf Breeze, FL 32561, USA
[d] Department of Atmospheric and Oceanic Sciences, University of California, Los Angeles, CA 90095, USA
[e] San Francisco Estuary Institute, Richmond, CA 94804, USA
[f] U.S. Geological Survey, Menlo Park, CA 94025, USA
[g] NOAA National Centers for Coastal Ocean Science, Silver Spring, MD 20910, USA
[h] Applied Marine Sciences, Santa Cruz, CA 95060, USA

ARTICLE INFO

ABSTRACT

San Francisco Bay (SFB), USA, is highly enriched in nitrogen and phosphorus, but has been resistant to the classic symptoms of eutrophication associated with over-production of phytoplankton. Observations in recent years suggest that this resistance may be weakening, shown by: significant increases of chlorophyll-*a* (*chl-a*) and decreases of dissolved oxygen (DO), common occurrences of phytoplankton taxa that can form Harmful Algal Blooms (HAB), and algal toxins in water and mussels reaching levels of concern. As a result, managers now ask: what levels of *chl-a* in SFB constitute tipping points of phytoplankton biomass beyond which water quality will become degraded, requiring significant nutrient reductions to avoid impairments? We analyzed data for DO, phytoplankton species composition, *chl-a,* and algal toxins to derive quantitative relationships between three indicators (HAB abundance, toxin concentrations, DO) and *chl-a*. Quantile regressions relating HAB abundance and DO to *chl-a* were significant, indicating SFB is at increased risk of adverse HAB and low DO levels if *chl-a* continues to increase. Conditional probability analysis (CPA) showed *chl-a* of 13 mg m^{-3} as a "protective" threshold below which probabilities for exceeding alert levels for HAB abundance and toxins were reduced. This threshold was similar to *chl-a* of 13–16 mg m^{-3} that would meet a SFB-wide 80% saturation Water Quality Criterion (WQC) for DO. Higher "at risk" *chl-a* thresholds from 25 to 40 mg m^{-3} corresponded to 0.5 probability of exceeding alert levels for HAB abundance, and for DO below a WQC of 5.0 mg L^{-1} designated for lower South Bay (LSB) and South Bay (SB). We submit these thresholds as a basis to assess eutrophication status of SFB and to inform nutrient management actions. This approach is transferrable to other estuaries to derive *chl-a* thresholds protective against eutrophication.

© 2017 Elsevier Ltd. All rights reserved.

1. Introduction

Nutrient over-enrichment has led to multiple ecosystem impairments of the world's estuaries (Nixon, 1995; Paerl, 1997; Cloern, 2001; Diaz and Rosenberg, 2008; Bricker et al., 2007). Identifying specific water-quality goals for nutrients is challenging, however, as ecological responses to nutrients are complex and variable. San Francisco Bay (SFB) is an example of a nutrient-enriched ecosystem exhibiting this complexity (Cloern and Jassby, 2012). Long-term observations suggest that SFB has been resistant to commonly observed symptoms of nutrient over-enrichment, such as high phytoplankton biomass, harmful algal blooms (HAB), and low dissolved oxygen (DO). A number of factors have precluded widespread development of such symptoms in SFB, including high turbidity leading to light-limitation of primary productivity, vigorous tidal flushing and mixing that limit biomass accumulation and DO depletion, and rapid grazing by the large populations of filter-feeding bivalves (Cloern, 1982).

* Corresponding author.
  E-mail address: marthas@sccwrp.org (M. Sutula).

Recent evidence suggests resistance to nutrient over-enrichment in SFB may be weakening, including: (1) a three-fold increase of chlorophyll-*a* (*chl-a*) since 1999 in South Bay (SB) during summer-fall (Cloern et al., 2007), linked to increased light availability and a climate-driven trophic cascade that reduced grazing losses (Cloern and Jassby, 2012); (2) common occurrences of HAB taxa (Lehman et al., 2005; Cloern et al., 2005; Cloern and Dufford, 2005); and (3) DO depressions to < 5 mg L^{-1} in Lower South Bay (LSB; Shellenbarger et al., 2008). These observations motivated the development of *chl-a* thresholds for SFB to assess potential impairments associated with nutrient over-enrichment.

Phytoplankton biomass as *chl-a* is a useful indicator of nutrient over-enrichment with well-established links to adverse effects on water-quality. This pivotal water-quality property is commonly used to assess eutrophication in support of regulatory goals (Bricker et al., 2003; Zaldivar et al., 2008; Harding et al., 2014). While a wealth of scientific literature supports the use of *chl-a* to assess eutrophication, defining specific *chl-a* thresholds that distinguish protective levels from those corresponding to risk of impairment is challenging. Quantitative thresholds can be based on deviations from "reference" conditions if data prior to degradation are available (Andersen et al., 2010, 2015), or on ecosystem impairments such as HAB, low DO, or water clarity (cf. Harding et al., 2014). Unfortunately, *chl-a* data are not available for SFB prior to human disturbance, limiting use of a reference approach. However, observations over the past three decades can be used to derive quantitative relationships between *chl-a* and adverse effects on water quality.

Two pathways linking nutrient over-enrichment to adverse effects on humans, marine mammals, and other aquatic life include: (1) increasing HAB abundance and toxins; and (2) low DO associated with excess organic matter production (Rosenberg et al., 1991; Diaz and Rosenberg, 1995; Heisler et al., 2008). Factors other than nutrients affect HAB and DO, and causal relationships are documented for nutrient loadings, *chl-a*, hypoxia, and HAB. Such relationships have been used to derive thresholds for assessment frameworks (Bricker et al., 2003), and water quality criteria (WQC) for Chesapeake Bay relating adverse effects to increased *chl-a* (Harding et al., 2014). As in many estuaries, *chl-a* has increased significantly in SFB over the past 15–20 years (Cloern et al., 2007), manifested as a three-fold increase of summer concentrations in SB and LSB (Fig. 1), previously unobserved autumn blooms (Cloern and Jassby, 2012), and significant increases of *chl-a* in other sub-embayments. Despite upward trends of *chl-a* and reports of HAB (see Cloern et al., 1994), algal toxins have not been monitored routinely in SFB. To date, long-term data on *chl-a*, phytoplankton species composition, and DO for SFB have not been used to determine if risks of HAB occurrences or low DO increase with increasing *chl-a*. We analyzed relationships between HAB, DO, and *chl-a* to derive quantitative *chl-a* thresholds protective from adverse effects. Our goals were: (1) to determine relationships of HAB occurrences, algal toxins, and DO to *chl-a*; and (2) to quantify *chl-a* thresholds and their uncertainties using statistical approaches that identified "protected" and "at risk" categories. These thresholds can be combined with HAB and DO data to assess status and trends in SFB that serve both scientists and managers (Sutula and Senn, 2017).

2. Materials and methods

2.1. Study area

SFB is the largest estuary in California, consisting of six sub-embayments (Fig. 1; Jassby et al., 1997). North Bay is river-dominated, with salinities ranging from 0 to 15. In contrast, South Bay is a marine lagoon, with salinities ranging from 5 to 35 ppt. The Sacramento and San Joaquin Rivers are the primary sources of freshwater to SFB, draining ~40% of California's landscape. The salinity distribution in North Bay changes with seasonal fluctuations in the Sacramento-San Joaquin discharge, while in South Bay salinity is also strongly influenced by wastewater discharge. Thirty-seven publicly owned wastewater treatment works (POTW) serving a population of 7.2 million dominate nutrient inputs to SFB. Most POTW perform secondary treatment without additional nitrogen (N) or phosphorus (P) removal. Runoff from the agricultural Central Valley and urban sources contributes to high nutrient inputs entering the northern SFB. Storm-water runoff from densely populated areas surrounding SFB also contributes to nutrient inputs. As a result, dissolved inorganic nitrogen (DIN) and ortho-phosphate (PO_4^{3-}) in SFB equal or exceed concentrations in other estuaries, such as Chesapeake Bay, where nutrient over-enrichment has led to degraded water and aquatic habitat (Cloern and Jassby, 2012).

2.2. Conceptual approach

Long-term data from the SFB Research Program of the US Geological Survey (USGS) and recent measurements of algal toxins supported analyses of DO and HAB trends. Relationships of DO and HAB to *chl-a* were used to derive *chl-a* thresholds corresponding to risks of low DO or HAB alerts. Several HAB taxa constitute part of the phytoplankton assemblage in SFB, with increased HAB occurrences corresponding to increased biomass as *chl-a*. For high-biomass HAB occurrences, significant relationships between HAB and *chl-a* supported development of WQC (Shutler et al., 2012; Schaeffer et al., 2012; Harding et al., 2014). Dominance by a particular taxonomic group, i.e., diatoms, expressed as cell counts or fraction of bio-volume, is often associated with high *chl-a*. Conditions leading to high *chl-a*, however, affect the entire phytoplankton community, not just HAB taxa (Barber and Hiscock, 2006), and we assumed increased *chl-a* reflected a broad increase of all phytoplankton, including potentially toxic HAB (Bricker et al., 2007; Glibert et al., 2005).

Microbial decomposition of phytoplankton biomass consumes DO, leading to hypoxia in conditions of excess substrate and vertical density stratification (Rabalais et al., 2014). Spatial and temporal displacement of high *chl-a* and DO depletion reflects seasonality of production and consumption (e.g., Wheeler et al., 2003), requiring empirical relationships that take account of relevant time and space scales. Accordingly, relationships between DO and *chl-a* were analyzed using data aggregated for a range of months, including varying temporal lags to capture production and metabolism of phytoplankton biomass.

2.3. Data sources

2.3.1. Cruises

We analyzed data collected from 1993 to 2013 by the USGS along a 145-km transect between the lower Sacramento River and LSB. All data are available online (Cloern and Schraga, 2016). At each station (Fig. 1), vertical profiles of DO were measured with Seabird SBE 13 (1993–2001) and SBE 43 (2002–2013) sensors, and *chl-a* with Sea Tech (1993–2001) and Turner Designs SCUFA fluorometers (2002–2013). The DO sensors and fluorometers were calibrated with ~20 discrete measurements per transect. DO was determined by Winkler titration and *chl-a* by fluorometric analyses of 90%-acetone extracts of water samples collected on GF/F filters. Depth-averaged DO and near-surface (≤2 m) *chl-a* data were aggregated as mean values for each of the six sub-embayments (Fig. 1). These were LSB (stations 34–36); SB (stations 24–32); Central Bay (CB, stations 20–23); North Central Bay (NCB, stations
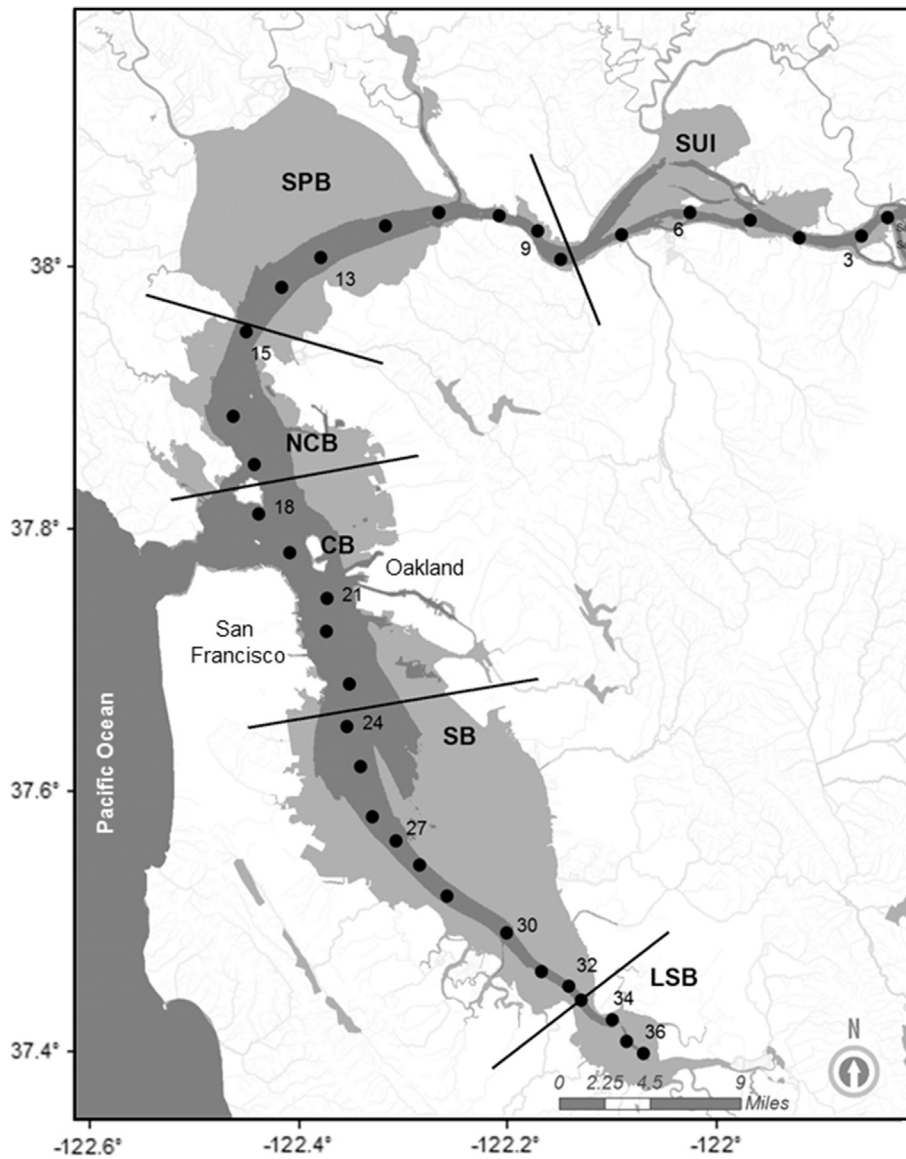
Fig. 1. Map of the San Francisco Bay system showing locations of USGS sampling stations (filled circles) and demarcation of six sub-embayments: Suisun Bay (SUB), San Pablo Bay (SBP), North Central Bay (NCB), Central Bay (CB), South Bay (SB), and Lower South Bay (LSB). Station 657 is a Delta station, not shown on map.

16—18); San Pablo Bay (SPB, stations 10—15); and Suisun Bay (SUB, stations 4—8). Data were aggregated for larger areas in some analyses to obtain bay-wide metrics, and to increase sample sizes for uncommon, but potentially deleterious HAB taxa.

Algal toxins, domoic acid (DA) and microcystin (MCY), were collected on Solid Phase Adsorption Toxin-Tracking (SPATT) samplers (Mackenzie et al., 2004) using samplers deployed in the flow-through system of the USGS *R/V Polaris* (~1 m intake) from October 2011 to November 2014. Transects encompassed LSB, SB, and CB (stations 18—36), LSB and SB (stations 24—36), NCB (stations 16—21), SPB (stations 9—15), and SUB and the lower Sacramento River (stations 4—8 and 657). Data were binned by sub-embayment, with SB and South-CB defined as stations 24—36 and 18—36. Operation of SPATT samplers was described previously for DA and MCY (Lane et al., 2010; Kudela, 2011; Gibble and Kudela, 2014), and reported as the total of congeners MCY-LR, MCY-RR, MCY-YR, and MCY-LA and DA. We placed 3 g Diaion HP20 resin in 100 μm Nitex mesh to create a SPATT sampler, and inserted them in the flow-through system for a defined spatial/temporal region. SPATT

samplers were frozen following deployment and processed in the laboratory. Extractions from SPATT used 50% methanol with analysis on an Agilent 6130 LC/MS in Selected Ion Monitoring mode. Calibrations consisted of analytical standards with SPATT toxins reported as weighted averages in units of ng toxin g^{-1} resin. Since SPATT is a passive sampling device, a direct extrapolation to volume of water sampled is not possible. Indirect estimation of ranges of *in situ* HAB toxins associated with SPATT concentrations has been documented (Kudela, 2011).

2.3.2. HAB abundance and toxins

HAB taxa were identified and counted in preserved samples by light microscopy. Seasonal and inter-annual distributions were determined for the three most common HAB taxa, *Pseudo-nitzschia sp.*, *Alexandrium sp.*, *Dinophysis sp.*, and others including *Heterosigma akashiwo*, *Karenia mikimotoi*, *Karlodinium veneficum*, and cyanobacteria *Microcystis, Oscillatoria, Planktothrix, Anabaenopsis*, and *Anabaena*. As there are no established alert levels for HAB in SFB, we relied on literature values and data from monitoring

programs. These alert levels included 10^6 cells L^{-1} for cyanobacteria (WHO, 2003), presence/absence for *Alexandrium* (http://www.scotland.gov.uk/Publications/2011/03/16182005/37), 10^2 - 10^3 cells L^{-1} for *Dinophysis spp.* (http://www.scotland.gov.uk/Publications/2011/03/16182005/37; Vlamis and Katikou, 2014), and 1–5×10^5 cells L^{-1} for *Pseudo-nitzschia.* Alert levels have not been established for *H. akashiwo, K. mikimotoi,* or *K. veneficum,* so we used 5×10^5 cells L^{-1} based on expert opinion and documented impacts in other regions (White et al., 2014; Silke et al., 2005; A. Place, pers. comm). Alert levels using SPATT have not been defined. Laboratory calibrations and studies at the Santa Cruz Municipal Wharf and Pinto Lake in California were used to establish alert levels of 1 ng g^{-1} for MCY produced by some cyanobacteria, and 75 ng g^{-1} for DA produced by *Pseudo-nitzschia* (Lane et al., 2010; Kudela, 2011; Gibble and Kudela, 2014).

2.4. Statistical analyses

Statistical analyses included: (1) seasonal Mann-Kendall tests to quantify trends of DO, HAB and *chl-a*; (2) ordinary least squares regression (OLS), and quantile regression to determine relationships of HAB, DO, and *chl-a*; and (3) quantile regression and conditional probability analyses (CPA) to derive quantitative thresholds for *chl-a* based on increased risk of HAB cell abundances that would trigger HAB alerts or a failure to achieve DO benchmarks. Quantile regression was used to determine *chl-a* concentrations associated with the 90th and 50th (median) quantiles of HAB abundances and 50th and 10th quantiles for DO. Quantile regression is analogous to rank-based correlation in that estimates are robust to extreme values, and do not require assumptions about distributions of residuals (Cade and Noon, 2003). CPA was used to analyze risk of HAB abundances above alert levels based on *chl-a* higher than a specified concentration, or of DO below WQC (R package *CProb*; Hollister et al., 2008). CPA generates the probability of an event, such as presence of HAB organisms above a defined threshold, given the occurrence of some other conditional event, such as *chl-*a at a specified concentration. It requires a dichotomous variable (in this case, harmful algal taxa above or below defined thresholds) and a continuous or discrete conditional variable (in this case, *chl-*a). Baseline probability, or the unconditional probability, represented the overall probability of an exceedance without regard to *chl-a* (i.e., *chl-a* > minimum concentration). Inflection points were interpreted as *chl-a* concentrations above which probability of an adverse HAB or DO event increased faster than increases of *chl-a*. We defined probability 0.5 as a benchmark for "elevated risk" as above this level an adverse event is more likely to occur than not. Results from CPA include confidence intervals based on bootstrapped calculations using 100 iterations for each CPA.

2.4.1. Statistical analyses of HAB − chl-a

HAB abundances and toxins were analyzed in the context of seasonal and inter-annual patterns of *chl-a* using near-surface samples. All cell counts for known HAB were used regardless of depth, and 24 of 1050 samples were deeper than 2 m, with 3 samples at a maximum depth of 35 m. USGS enumerated phytoplankton for samples with *chl-a* $\geq$ 5 mg m^{-3}, possibly introducing sampling bias by neglecting HAB at low *chl-a*. Another bias was the lack of records for *Microcystis* spp., suggesting these cells were not identified by microscopy although they are regularly observed in northern SFB.

Relationships of HAB abundances and SPATT toxin to *chl-a* with OLS and quantile regressions were conducted on log_{10}-transformed data to achieve normality (Campbell, 1995). We compared HAB abundances and SPATT toxin to mean or maximum *chl-a* from corresponding sub-embayments. HAB alert levels (see above) were used to derive probabilities that HAB or toxins would reach problematic levels as *chl-a* increased. Selection of alert level influenced the probability derived from CPA (see below).

Quantile regression and CPA were used to identify *chl-a* thresholds based on the risks of exceeding alert levels for HAB abundance or toxins. Steps included: (1) CPA on HAB abundance and SPATT toxin aggregated for all sub-embayments; a "HAB event of concern" was a site where at least one HAB taxa exceeded alert levels based on abundance; (2) quantile and OLS regressions to quantify relationships between abundances of *Alexandrium, Dinophysis, Heterosigma, Karlodinium,* and *Pseudo-nitzschia* and *chl-a*. Corresponding analyses were performed for SPATT toxin aggregated for years and sub-embayments. Analyses were also conducted with and without *Alexandrium,* a toxic genus with the potential to introduce sampling bias because it has a low alert level. Concern that relationships between HAB and *chl-a* might be affected by HAB from coastal waters led us to conduct CPA on data aggregated by sub-embayment; (3) data were sorted into pre- and post-2002 periods to examine decadal differences.

2.4.2. Statistical analyses of DO - chl-a

Near-surface data from USGS cruises were used to derive relationships between DO and *chl-a*. Mean, seasonal *chl-a* was calculated for periods when *chl-a* has increased, including: (1) spring bloom (February–May); (2) summer baseline (June–September); and (3) both periods (February–September) (Cloern et al., 2007). Mean *chl-a* from February–September was used to derive thresholds of risk of low DO based on OLS. Evaluation periods were based on existing WQC for DO, consisting of: (1) instantaneous DO > 7 mg L^{-1} upstream and >5 mg L^{-1} downstream of the Carquinez Bridge, not to fall below these values more than 10% of the time (SFRWQCB, 2015); and (2) > 80% DO saturation for the running three-month median in any sub-embayment. Median percent DO saturation and DO concentration (mg L^{-1}) were computed from vertical profiles. Stations with DO failing to meet the WQC were enumerated by sub-embayment. Three-month intervals with the most DO exceedances were subjected to further statistical analyses as these periods are susceptible to low DO.

Quantile regressions of the relationships between DO and *chl-a* by sub-embayment considered several time lags to investigate the time scales at which spring biomass production is linked to DO consumption in the summer (Hagy et al., 2004). We used % DO saturation to remove effects of temperature and salinity on oxygen solubility. Median (i.e., $\tau = 0.5$) quantiles of % DO saturation were used to test significance of relationships between DO and *chl-a* for three periods. For sub-embayments with significant negative relationships between DO and *chl-a*, thresholds of increased risk of falling below DO benchmarks were quantified using two approaches. First, quantile regression using $\tau = 0.1$ was used to identify the mean and 95% confidence intervals of *chl-a* concentrations at which % DO saturation of 80%, 72%, 57%, and 46% would be expected 90% of the time. These % DO saturation values are equivalent to DO concentrations of 7.0, 6.3, 5.0 and 4.0 mg L^{-1} at $15°$ C and salinity 24. Selection of $\tau = 0.1$ (i.e., 10% non-attainment) corresponds to California State Water Resource Control Board guidance for listing of impaired waters (SFRWQCB, 2015). Benchmark DO concentrations of 6.3 and 5.0 mg L^{-1} are the lowest DO concentrations to which salmonid and non-salmonid fish, respectively, can be exposed indefinitely without exhibiting >5% impact
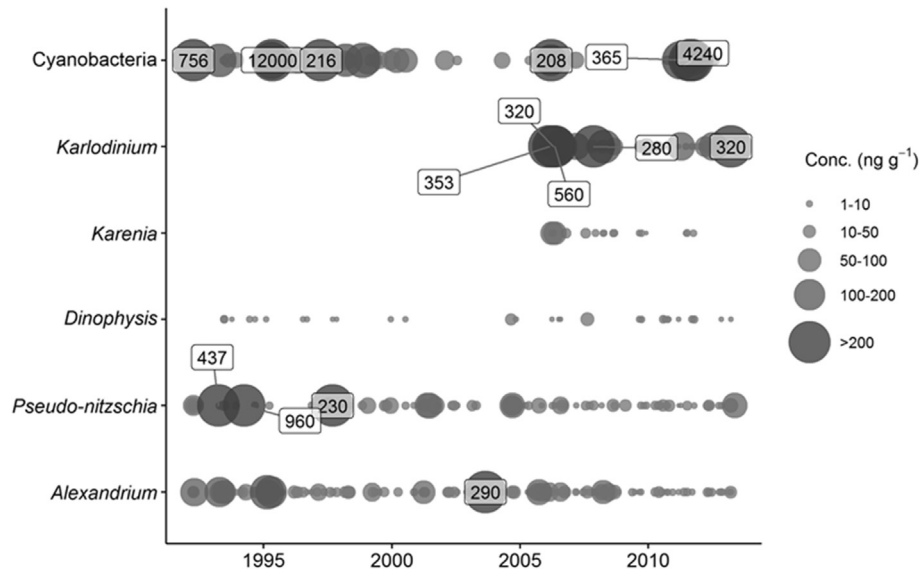
Fig. 2. Abundances of six HAB taxa in SFB from 1993 to 2014. Symbols indicate abundance (cells mL^{-1}) by cruise. The station with the highest cell density is indicated for cruises with HAB enumerated at multiple locations. Inset values give abundance at stations >200 cells mL^{-1}.

to estuarine populations (Bailey et al., 2014). Benchmarks of 7.0 and 5.0 mg L^{-1} are the established WQC for DO in sub-embayments of SFB. We also used CPA to identify *chl-a* concentrations corresponding to % DO saturation that met a WQC for median, three-month % DO saturation of 80% half the time ($\tau = 0.5$). Lastly, CPA was used to identify change points in the probability of DO falling below established WQC for DO as a function of increasing *chl-a*.

3. Results

3.1. HAB abundance and algal toxins

HAB taxa were detected in ~50% of samples and abundances exceeded alert levels in ~35% of samples. Of samples exceeding alert levels, 53% contained *Alexandrium,* 11% *Dinophysis*, and 7%
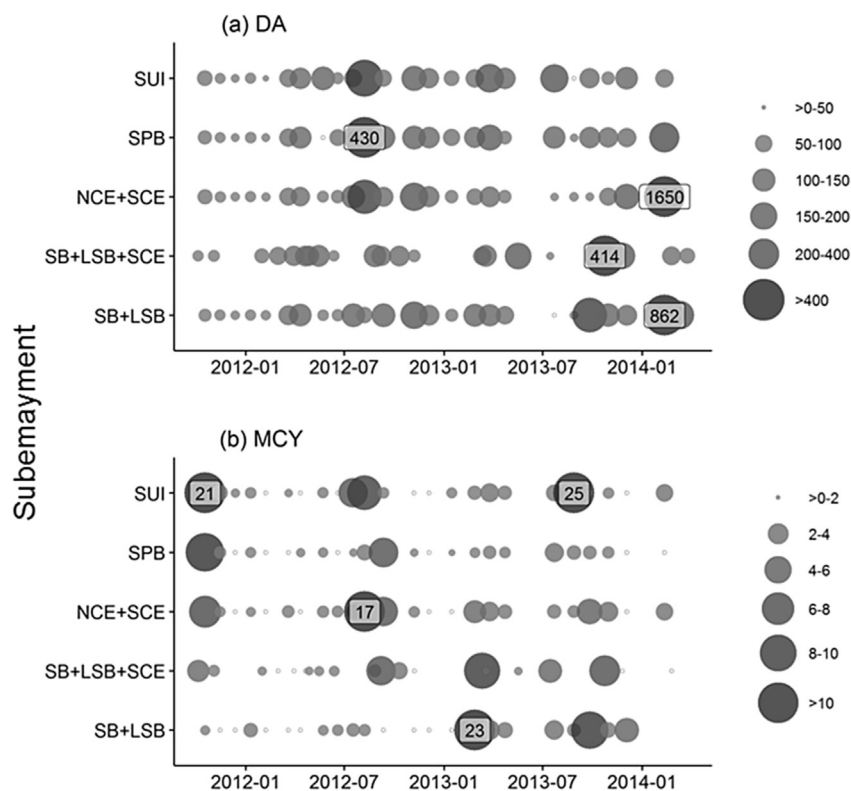

Fig. 3. Concentration (ng g^{-1}) of (a) domoic acid DA (ng g^{-1}) and (b) microcystin MCY (LR, RR, YR, and LA) in from SPATT deployed in the R/V *Polaris* surface mapping system for regions representing the following sub-embayments: SUB + Delta station, SPB, NCB, and SB + CB during full Bay cruises, and LSB + SB during South SFB only cruises sub-embayments. Labeled circles indicate samples where DA > 400 ng g^{-1} and MCY >10 ng g^{-1}.

Pseudo-nitzschia (Fig. 2). Algal toxins collected by SPATT revealed common occurrences of DA and MCY (Fig. 3). Of 158 SPATT samplers deployed, 72% showed detectable MCY and 97% showed detectable DA. Mean toxin concentrations in SPATT were 0.75 ng g^{-1} for MCY and 57 ng g^{-1} for DA, with detectable toxin ranging from 0.01 to 25.5 ng g^{-1} for MCY, and from 1.69 to 1650 ng g^{-1} for DA (Fig. 3a–b). Suggested guidelines of 1 ng/g for MCY and 75 ng/g for DA indicate that the average concentrations of both toxins are below levels of concern for acute toxins, but both toxins exceeded these thresholds by an order of magnitude in some samples, suggesting that toxins sporadically exceed levels of concern (see also Figs. 2 and 3).

3.2. DO, HAB abundance, algal toxins, and chl-a

Significant trends of decreasing DO and increasing *chl-a* from 1993 to 2013 were found in all sub-embayments using a seasonal Mann-Kendall test (all *p* < 0.05). Summer *chl-a* increased significantly throughout SFB, with largest increases in central and southern sub-embayments (Fig. 4). Trends from Mann-Kendall tests ranged from −0.9 to −1% DO saturation yr^{-1} and 0.041–0.096 mg *chl-a* m^{-3} yr^{-1}. HAB taxa showed no significant increases based on Kendall's Tau test (p > 0.1). Cell counts for

Pseudo-nitzschia or *Alexandrium* analyzed by sub-embayment showed no significant trends (ANCOVA, p > 0.05). The 10th percentile of summer DO ranged from 5.7 to 7.8 mg L^{-1} on south to north transects (Supplemental Material, Table S1 and Fig. S1). DO was >5 mg L^{-1} from 97.1 to 100% of the time along these transects, with DO > 7 mg L^{-1} in SUB 100% of the time. For most sub-embayments, evaluation periods with DO below the WQC using the three-month running median of 80% saturation were May–July and June–August (Supplemental Material, Table S2), and data from these periods were used in quantile regressions.

3.3. Relationships of HAB and chl-a

Relationships of HAB abundance and SPATT toxin to *chl-a* showed considerable scatter. Abundances of *Alexandrium*, *Dinophysis*, *Karlodinium*, and *Pseudo-nitzschia* increased with increasing *chl-a* and slopes of median quantile regressions ($\tau = 0.5$) were significant (all *p* < 0.05). Slopes and [R^2] of quantile regressions of abundance on *chl-a* for these genera were 0.48 [0.25], 0.56 [0.33], 1.4 [0.44], and 0.43 [0.45], respectively, in units of log-transformed cell density divided by log-transformed *chl-a*. Cyanobacteria, *Heterosigma*, and *Karenia* showed no significant relationships with *chl-a*. SPATT toxin analyzed by sub-embayment showed a significant
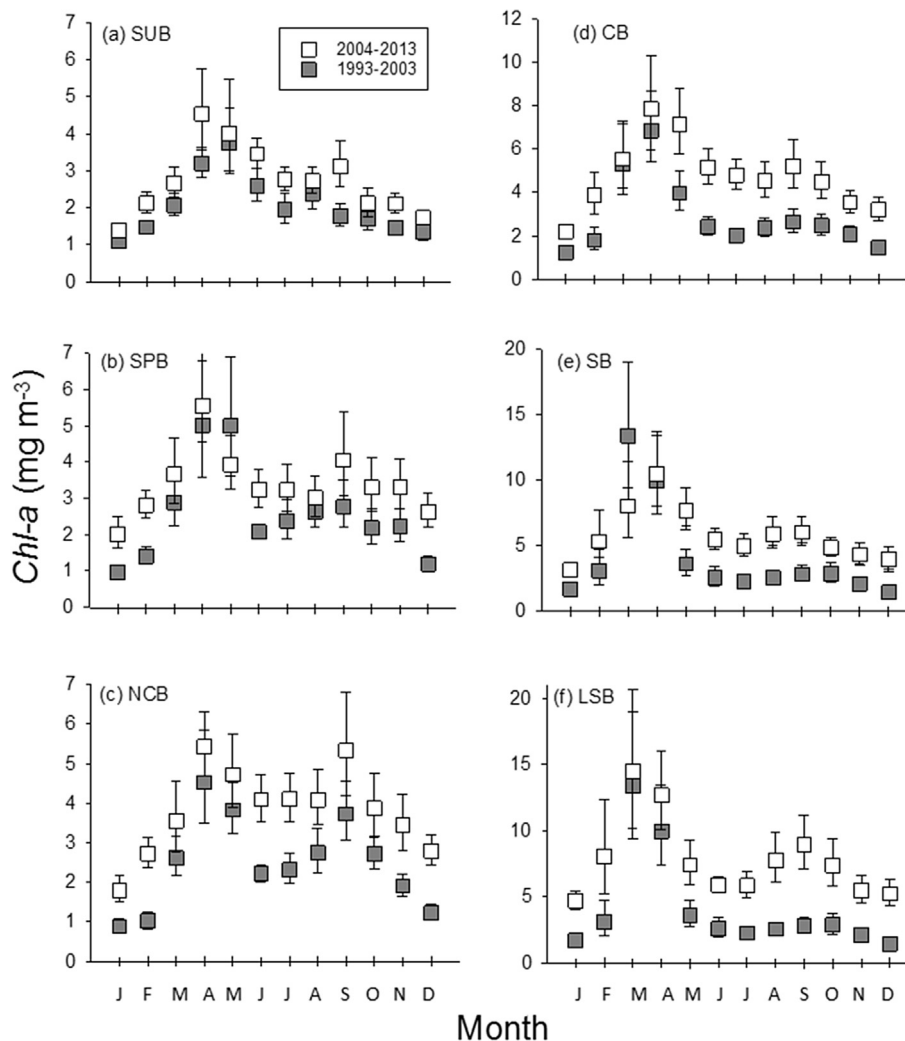

Fig. 4. Monthly geometric mean and 95% confidence interval of *chl-a* comparing the periods 1993–1999 and 2000–2014, by sub-embayment, from north to south, (a) SUB, (b) SPB, (c) NCB, (d) CB, (e) SB, and (f) LSB. An abrupt increase of *chl-a* occurred after 1999 coincident with a shift of the NE Pacific to its cool phase (Cloern et al., 2007).

Table 1

Slopes of quantile regressions at Tau = 0.1 and 0.5 by DO integrating period (May–July and June–August) and *chl-a* averaging period (February–May, June–September, and February–September). Significance levels: *p < 0.1, **p < 0.05, ***p < 0.01.

Subembayment and DO Integrating Period	Slope of Quantile Regressions and Significance Level					
	February–May Mean		June–September Mean		February–September Mean	
	0.1 Tau	0.5 Tau	0.1 Tau	0.5 Tau	0.1 Tau	0.5 Tau
May–July						
LSB	0.06	−0.04	−0.22	−0.62**	−0.73**	−0.61**
SB	−0.38***	−0.28***	−0.17	−0.58***	−0.78***	−0.73***
CB	−0.43	0.01	2.15***	0.74**	−0.73	0.15
NCB	−0.20	0.14	1.18	0.87	−0.84	0.85
SPB	−0.36	−0.44	−0.93	−0.58***	−0.77	−0.37
SUB	−0.85	−0.57	−0.86	−0.45	−1.99***	−0.16
June–August						
LSB	−0.14	−0.23***	0.62	0.39	−0.14	−0.20
SB	−0.29***	−0.17***	0.16	−0.02	−0.60***	−0.39***
CB	−0.47	−0.10	0.74*	0.70**	0.27	0.27
NCB	−0.25	−0.13	0.98	0.60	0.39	0.39
SPB	−0.20	−0.11	−0.11	−0.36*	−0.33	−0.33
SUB	0.02	0.05	−1.08	−0.82	0.49	−0.49

increase of MCY and DA with increasing mean *chl-a*, and a significant increase of DA with maximum *chl-a*.

3.4. Relationships of DO and chl-a

Quantile regressions of median DO in May–July, June–August or February–September on mean, seasonal *chl-a* were similar, with negative slopes for SUB, SPB, SB, and LSB, regardless of the averaging period for *chl-a* (Table 1; Fig. 5). Slopes were steepest and most highly significant for regressions on mean, seasonal *chl-a*, February–September. Slopes of regressions of median DO on mean, seasonal *chl-a* from June–September were negative and significant (all $p < 0.05$) for SPB, SB, and LSB, while analogous relationships to mean, seasonal *chl-a* from February–May were negative and significant when correlated with SB and LSB (Table 1). Slopes of quantile regressions of median DO on mean, seasonal *chl-a* were not significant (all $p > 0.05$) for CB and NB. The slopes of the regressions for SPB were significant ($p < 0.001$), but observations at high *chl-a* were uncommon and the relationships were sensitive to outliers (Fig. 5). Data for NB and CB had insufficient exceedances of WQC for DO to conduct CPA. Thus derivations of DO-based *chl-a* thresholds were limited to SB and LSB.

3.5. Thresholds based on chl-a

3.5.1. HAB relationships to chl-a

The baseline probability of HAB occurrences for the full range of *chl-a* was 0.35–0.40 (Fig. 6). This implies that 35–40% of all samples exceeded HAB alert levels based on abundance. Mean probability of exceeding HAB alert levels 50% of the time corresponded to *chl-a* > 37.5 mg m^{-3} with an upper 95% confidence interval of 13.5 mg m^{-3}. An inflection point for probability corresponding to increased risk occurred at *chl-a* > ~25 mg m^{-3}. The *chl-a* thresholds derived with CPA were consistent with relationships of HAB to *chl-a* using quantile regressions, with a 0.50 probability of HAB corresponding to a broad range of *chl-a* between 3.5 and 40 mg m^{-3}. Low-biomass, highly toxic genera such as *Alexandrium* and *Dinophysis* occupied the low end of the *chl-a* range, while high-biomass taxa such as *Heterosigma* and *Pseudo-nitzschia* occurred at the high end. CPA for individual sub-embayments were affected by sample size and relatively few observations at high *chl-a*, but spatially aggregated data identified similar thresholds. Exceptions included NCB and CB that showed flat relationships with *chl-a* (see Fig. 7). Other sub-embayments showed increased probabilities of HAB with

increasing *chl-a*, exceeding 0.80 at highest *chl-a* in SPB and SB. More than 90% of the observations in NB and CB occurred at *chl-a* < 13 mg m^{-3}, while *chl-a* > 13 mg m^{-3} occurred commonly only in SB and LSB (18% and 26%, respectively; Supplemental Materials, Fig. S2).

OLS regressions of SPATT toxin on *chl-a* were not statistically significant, but CPA on toxins and *chl-a* gave similar inflection points as we derived for HAB (Fig. 8). The baseline probability for DA began at ~0.35 for the full range of *chl-a*, and increased to ~0.6 at *chl-a* > 13 mg m^{-3} (Fig. 8a). A similar pattern was observed for MCY with a baseline probability of ~0.3 (Fig. 8b). Very few SPATT observations exceeded *chl-a* thresholds for HAB alert levels (>13 mg m^{-3}), but an increased probability of exceeding toxin thresholds at *chl-a* > 10 mg m^{-3} was consistent with the probability of exceeding alert levels for HAB abundance using CPA (Fig. 6).

3.5.2. Thresholds relating DO to chl-a

Quantile regressions of DO from May–July on mean, seasonal *chl-a* in SB and LSB showed significant, negative slopes for $\tau = 0.1$ and 0.5 for *chl-a* averaged over three periods (Fig. 5c–d, see p-values and slopes, Table 1). Slopes were steeper and more significant for DO from May–July than from June–August. Based on quantile regressions for SB using DO from May–July, mean *chl-a* of 14 mg m^{-3} during February–September was associated with a low frequency of DO below the WQC, while the frequency of low DO increased at *chl-a* ≥ 17 mg m^{-3} (Table 2). Comparison of *chl-a* for a gradient of DO concentrations was informative. Quantile regression predicted 90% of DO concentrations would exceed 7 mg L^{-1} at *chl-a* of 14 mg m^{-3}, while 90% of DO would exceed 5.0 mg L^{-1} at *chl-a* ≥ 42 mg m^{-3} (Table 2). As context, 95% of mean, seasonal *chl-a* from February–September were <14 mg m^{-3} in SB from 1993 to 2014 (Supplemental Materials, Fig. S2).

DO was predicted to fall below WQC at lower *chl-a* in LSB than in SB, although the confidence intervals were larger for LSB. At mean, seasonal *chl-a* of 16 mg m^{-3} from February–September, we identified elevated risk of DO below a WQC specified as a three-month median DO saturation of 80% (Table 2). A 10% probability of DO below the WQC was associated with *chl-a* of 4 mg m^{-3}. This suggests advection of DO-depleted water into the study area from adjacent, highly productive habitats with documented hypoxia produced a high probability of DO below the WQC even at low *chl-a*. Similarly, CPA showed a baseline probability of 0.2 of DO below the WQC (Fig. 9). This baseline was moderately high considering a mean probability of 0.5 based on the WQC for DO at *chl-a* >
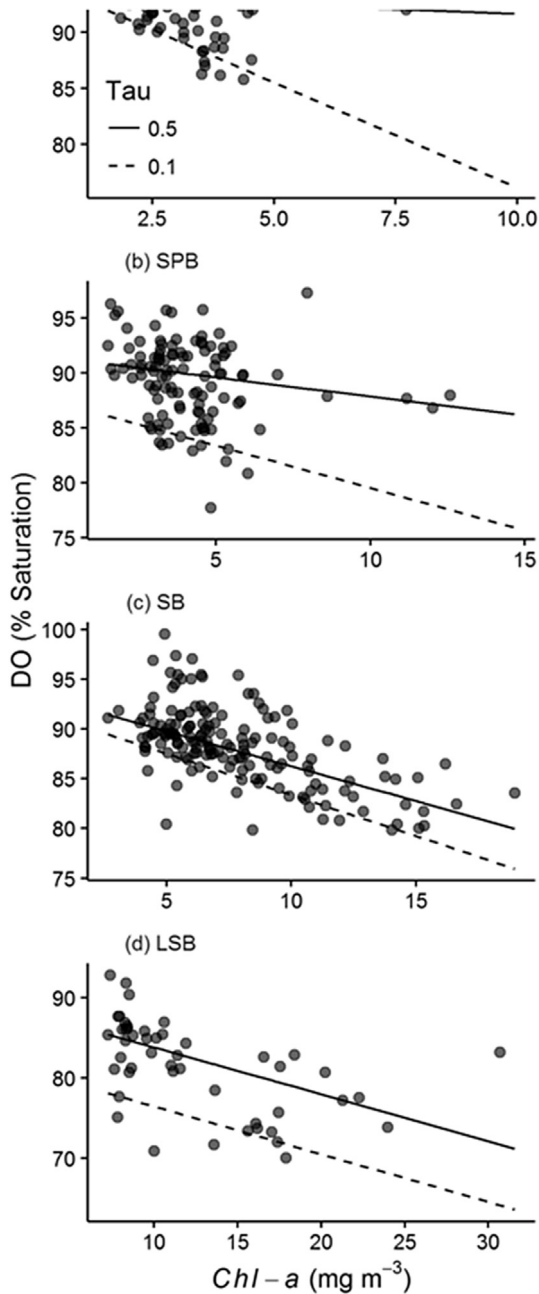
Fig. 5. Comparison of quantile regressions relating % DO saturation from May–July to mean *chl-a* from February–September in four sub-embayments: (a) SUB, (b) SPB, (c) SB, (d) LSB. Lines for the 10th ($\tau = 0.1$, dashed line) and median ($\tau = 0.5$, solid line) quantiles are shown. Summary of correlation and significance levels of regression analyses is given in Table 1.

14 mg m^{-3}, with an upper 95% confidence interval >10 mg m^{-3}. These findings suggest mean *chl-a* at or above these thresholds carries increased risk of DO falling below the WQC (Fig. 9). Applying CPA and comparing results to DO and *chl-a* distributions in SFB, we observed that 90% of DO concentrations would exceed 6.3 mg L^{-1} and 5.0 mg L^{-1} at *chl-a* of 15 mg m^{-3} and 36 mg m^{-3}, respectively (Table 2). Long-term data showed 95% of the February–September mean *chl-a* in LSB was <25 mg m^{-3} (Supplemental Materials, Fig. S2), and low DO associated with high *chl-a* remains uncommon in the open channel habitat of LSB.
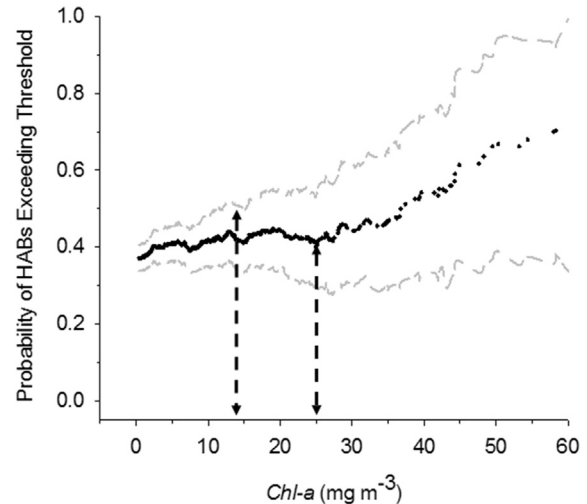

Fig. 6. Probability of a HAB cell density exceeding alert levels if a specified *chl-a* concentration is exceeded for data in which all HAB species are included. Grey dashed lines are lower and upper 95% confidence intervals of bootstrap values (100 iterations). Dashed arrows indicate: 1) a *chl-a* threshold of 13.5 mg m^{-3}, representing regions of the upper 95% confidence interval of 0.5 probability of exceeding HAB alert levels fifty percent of the time, and 2) an inflection point for probability corresponding to increased risk of HABs at *chl-a* > ~25 mg m^{-3}.
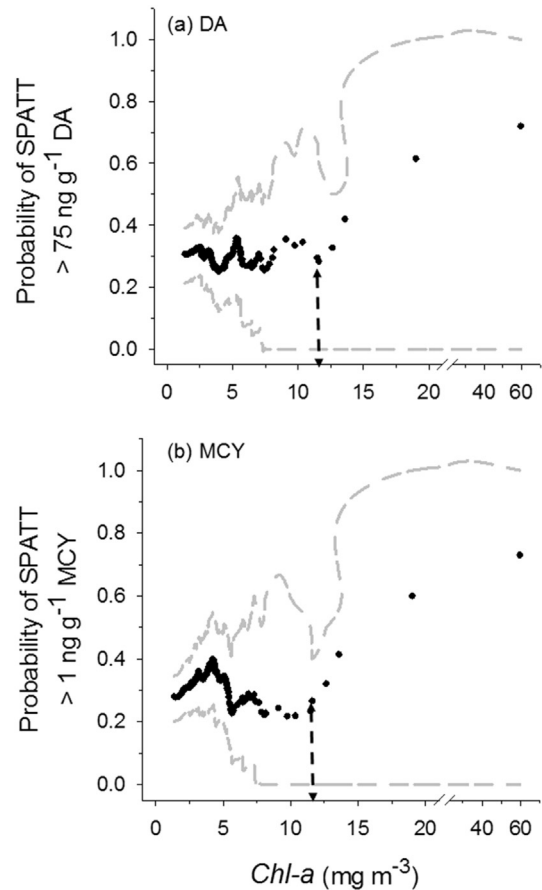

Fig. 7. Probabilities of DA (top panel) or MCY (bottom panel) > 75 ng g^{-1} and 1 ng g^{-1}, respectively, indicating risk when specified monthly *chl-a* concentrations are exceeded. The black line represents mean probability. Dashed lines are lower and upper 95% confidence intervals from bootstrap (100 iterations). Dashed arrows show inflection points for probability corresponding to increased risk at *chl-a* > ~13 mg m^{-3}.
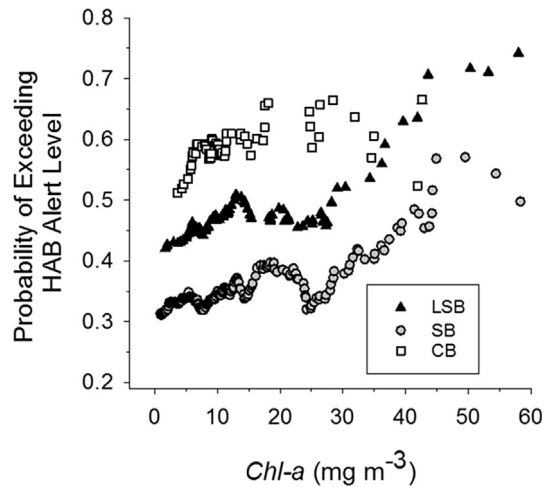
Fig. 8. Mean probability of any HAB species exceeding its alert level if a specified monthly *chl-a* concentration is exceeded, by sub-embayment for CB (open squares), SB (black triangle), and LSB (grey circle).
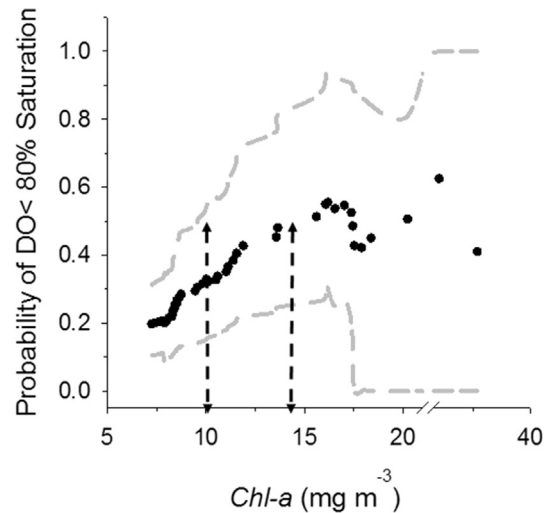

Fig. 9. Probability of DO percent saturation <80% during the months of June–August in LSB as a specified February–September mean *chl-a* concentration is exceeded. The black line represents mean probability. Grey dashed lines are lower and upper 95% confidence intervals of bootstrap values (100 iterations). Dashed lines indicate: 1) threshold of >10 mg m^{-3} representing the upper 95% confidence interval of 0.5 probability of not meeting the DO WQC and 2) threshold of the mean 0.5 probability of not meeting the WQC at *chl-a* > 14 mg m^{-3}.

4. Discussion

4.1. Current status and potential for eutrophication in SFB

Human activities have led to nutrient over-enrichment of bays and estuaries by N and P, but ecosystem responses show high spatial and temporal variability (Cloern, 2001), and exhibit sensitivity to climate variability and change (Cloern et al., 2015; Harding et al., 2015). Nutrient over-enrichment commonly culminates in environmental degradation associated with the accumulation of excess phytoplankton biomass as *chl-a*. A number of factors, such as physical transport, vertical density stratification, residence time, light availability, floral composition, and grazing, determine if deleterious impacts are realized by modulating the conversion of nutrients into biomass. Nutrient concentrations are higher in SFB than in estuaries exhibiting water-quality degradation, but DO is higher and *chl-a* is lower in SFB than in Chesapeake Bay, the Neuse River estuary, Seine Bay, and the Westerschelde where impairments are well documented (Bricker et al., 2007; Cloern and Jassby, 2008). Despite data indicating that DO and *chl-a* are less problematic in SFB than elsewhere, we report significant trends of decreasing DO and increasing *chl-a*, a ubiquitous presence of toxin-producing phytoplankton, and algal toxins at levels of concern. Increased light availability and reduced grazing pressure have contributed to increased *chl-a* (Cloern and Jassby, 2012), and deleterious ecosystem responses may occur in SFB in the future.

Chl-a thresholds that characterize the risk of adverse effects can help focus management attention and protect SFB from water-quality degradation that has occurred in other estuaries (Harding et al., 2015).

HAB abundance exceeded alert levels in ~35% of samples from SFB, documenting a potential for adverse effects on ecosystem health. HAB taxa are expected to occur at some baseline level, based on the cosmopolitan distributions of many species (Lundholm and Moestrop, 2006). However, data presented here showed the probability of HAB was high in SFB. The high baseline of occurrence we observed reflects strong connectivity with at least two sources of HAB seed populations. One source is the coastal ocean adjacent to SFB, a known source of toxic phytoplankton responsible for closures of shellfish harvesting (Lewitus et al., 2012) associated with a massive west-coast HAB event in 2015 (McCabe et al., 2016). A second source of HAB taxa is the salt ponds in SB and LSB, the dinoflagellates, *Alexandrium* spp. and *Karenia mikimotoi*, the raphidophyte, *Chattonella marina*, and cyanophytes, *Anabaenopsis* spp. and *Anabaena* spp. (Thébault et al., 2008). Recent samples from SB contained HAB taxa that were rarely observed prior to opening of the salt ponds a decade ago, among them *Karlodinium veneficum*,

Table 2
Comparison of mean and 95% confidence interval (CI; in parentheses) of predicted *chl-a* (mg m^{-3}) from quantile regressions of mean, seasonal *chl-a* from February–September, and DO for from May–July for specified DO benchmarks. 80% saturation at a $\tau = 0.5$ is equivalent to the WQC for % DO saturation in SFB. Predicted *chl-a* at $\tau = 0.1$ represents a 10% frequency of falling below a gradient of DO benchmarks from the literature (i.e., 80%, 72%, 66% and 57% saturation, corresponding to DO concentrations given in parentheses for mean summer temperatures of 15 °C and salinity of 24). All regressions were significant ($p < 0.05$).

DO % saturation, with Equivalent Concentration	Predicted Mean *chl-a* (95% CI)	
	LSB (N = 48)	SB (N = 161)
$\tau = 0.5$		
80% (~7 mg L^{-1})	15.6 (9.2–21.8)	17.3 (15.1–19.5)
$\tau = 0.1$		
80% (~7.0 mg L^{-1})	4.3 (−4.1–12.1)	14.3 (12.6–15.5)
72% (~6.3 mg L^{-1})	15.3 (5.3–29.3)	24.6 (21.9–24.7)
66% (~5.7 mg L^{-1})	23.5 (15.3–39.3)	32.3 (29.5–32.3)
57% (~5.0 mg L^{-1})	35.8 (30.3–54.3)	43.8 (40.5–45.9)
46% (~4.0 mg L^{-1})	50.9 (41.4–60.4)	57.9 (56.2–59.2)

Chattonella marina, and *Heterosigma akashiwo*. Abundances of *K. mikimotoi* and *K. veneficum* also increased in LSB and SB during that time interval. Spatial distributions of these HAB suggest a potential for invasion of other sub-embayments, with implications for ecosystem health of SFB (Thébault et al., 2008). Significant relationships of HAB cell densities to *chl-a* for a number of HAB taxa confirm SFB is a suitable habitat for potentially deleterious taxa, in part due to nutrient over-enrichment that underlies increased phytoplankton biomass.

HAB occurrences based on cell densities above defined alert levels indicate a potential threat, while detection of toxins confirms that threat by revealing that environmental conditions in SFB and connected habitats (i.e., marine, restored wetland, and/or Delta) support toxigenic phytoplankton. SFB is not routinely monitored for HAB toxins, and from 1994 to 2004 no acute wildlife mortalities or human illnesses were directly attributed to HAB occurrences. MCY has been linked to negative impacts on aquatic food webs in the Sacramento-San Joaquin Delta connected to SFB (Lehman et al., 2010), and there is increasing evidence that chronic, sub-lethal exposure to DA may be problematic (Goldstein et al., 2008; Montie et al., 2012). Specific findings from this study include cyanobacteria, that while not adequately enumerated in current sampling, produce the toxin MCY, and the diatom, *Pseudo-nitzschia*, a producer of the toxin DA, with cell densities above alert levels in ~11% of samples. Toxin measurements using SPATT showed measurable quantities of MCY and DA in 72% and 97% of SPATT deployments, confirming presence of toxigenic phytoplankton. SPATT detects low concentrations of toxins compared to traditional methods (Lane et al., 2010; Kudela, 2011), but analyzing SPATT data to exclude lowest toxin concentrations still showed ~35% of samples with toxins. Together, these findings demonstrate that dissolved toxins are widely distributed throughout SFB and are common throughout the year.

Significant relationships between HAB abundance and *chl-a* are established, but coincident observations of low DO and high *chl*-a were rarely observed in SFB and relationships differed greatly by sub-embayment. The lack of consistent, significant relationships between DO and *chl-a* in SUB, SPB and CB suggests physical processes precluded development of low DO, despite accumulations of high phytoplankton biomass (Smith and Hollibaugh, 2006). These factors appear effective in sub-embayments adjacent to the coastal ocean and the Sacramento/San Joaquin Delta, respectively. The relationship of DO to *chl-a* is quite different in LSB, a lagoonal sub-embayment with a long residence time adjacent to highly productive restored salt ponds (Thébault et al., 2008), and to tidal sloughs that experience hypoxia (Shellenbarger et al., 2008).

4.2. Chl-a as the basis to assess water-quality in SFB

Chl-a has been used to assess eutrophication in estuaries around the world (Bricker et al., 2003; Zaldivar et al., 2008). Our analyses related specific water-quality impairments in SFB to *chl-a*, consistent with published work that applies *chl-a* as an indicator of nutrient over-enrichment (Bricker et al., 2007; Devlin et al., 2011; Harding et al., 2014). Here, we have presented several key findings to support this approach. First, we documented significant relationships between HAB abundance, DO, and *chl-a* using quantile regressions. Results were consistent with a conceptual model of increased risk for problematic HAB abundance, toxins, and low DO at increased phytoplankton biomass (Cloern, 2001). Second, several statistical methods produced consistent ranges for *chl-a* thresholds based on HAB and DO. An inflection point of mean seasonal *chl-a* < 13 mg m^{-3} represented a threshold below which probabilities of increased HAB abundance and SPATT toxins decreased while the same *chl-a* threshold applied to a 3-month median DO would

consistently exceed at WQC of 80% saturation (~7 mg L^{-1} DO). At the opposite end of risk, 25–40 mg m^{-3} *chl-a* was associated with a heightened risk of HAB abundance and, in LSB and SB, excursions below DO of 5 mg L^{-1}.

The *chl-a* thresholds based on HAB and DO that we derived for SFB were similar to published thresholds for other ecosystems based on a variety of assessment methods. Harding et al. (2014) reported mean annual *chl-a* < 15 mg m^{-3} corresponded to decreased risk of *Microcystis* spp. toxins, and mean summer *chl-a* from 7.2 to 11 mg m^{-3} precluded low DO in deep waters of Chesapeake Bay. Bricker et al. (2003) designated *chl-a* ~20 mg m^{-3} as a threshold of "high" risk for eutrophication, a value agreed upon by expert judgment. Similarly, *chl-a* thresholds of 10, 20 and 50 mg m^{-3} were used to define "low", "high", and "very high" risk of eutrophication in the Phytoplankton Biological Quality Element for the European Union (EU) Water Framework Directive (WFD) (Devlin et al., 2011).

Nutrient inputs and phytoplankton responses are sensitive to hydrological variability in estuarine and coastal ecosystems, reflecting both climate forcing and climate change (Cloern et al., 2015). Recent studies document these responses for two large ecosystems, the Danish Coast (Riemann et al., 2015) and Chesapeake Bay (Harding et al., 2016). SFB is characterized by high ambient nutrient concentrations (Cloern and Jassby, 2012), indicating incomplete nutrient assimilation and a potential to support additional phytoplankton biomass, a response that would have significant water-quality implications. High N and P concentrations suggest the potential to stimulate phytoplankton growth and biomass, at levels comparable to levels leading to water quality impairments in other estuaries, such as Chesapeake Bay (Kemp et al., 2005). For example, median concentrations of dissolved inorganic nitrogen (DIN) from 2000 to 2014 were 31.4 and 57.5 μM in SB and LSB, respectively. The magnitude of median DIN in SB is such that phytoplankton can grow at ca. 95% of their maximum growth rate, assuming a half saturation constant of 1.5 μM. Concentrations of PO_4^{3-} relative to phytoplankton growth requirements are even higher. Therefore, biomass production in SFB is not limited by nutrients, and its potential for accumulation is high. That high biomass production has not been observed because it is constrained by other factors, such as high turbidity and fast grazing by benthic filter feeders (Cloern, 2001). However, we have learned from observations in other estuaries that these constraining factors may change abruptly over time, leading to surprisingly large increases or decreases of biomass (Duarte et al., 2009; Raimonet and Cloern, 2017). This heightened risk for biomass accumulation is a strong motivation for managers to consider establishing *chl-a* thresholds for SFB.

4.3. Chl-a thresholds in the context of managing risk

Environmental management and regulation are firmly grounded in a risk assessment paradigm (US Environmental Protection Agency, 1998). For this reason, evaluating risk is a useful point of departure to derive *chl-a* thresholds as a basis for assessing nutrient over-enrichment of SFB (Sutula and Senn, 2017). Here, we used CPA and quantile regression to derive *chl-a* thresholds corresponding to low and high risk of exceeding HAB alert levels. A similar approach has been used to derive water-quality goals for freshwater ecosystems (Paul and McDonald, 2005), though fewer applications exist for the marine environment. CPA and quantile regression produced estimated probabilities of negative outcomes, conditional upon water-quality measures, a key element of environmental decision-making (National Research Council, 2009).

Statistical approaches relating HAB and DO to *chl-a* quantified uncertainties, two sources of which should be considered when

applying *chl-a* thresholds to nutrient management and ecosystem assessment. First, the significance of HAB in SFB for ecosystem and human health is unknown and additional data are needed on bio-accumulation of toxins, acute and chronic toxicity to the biota, and risk to human health and aquatic life. Differences among sub-embayments indicate that relationships between HAB toxins and *chl-a* should take into account spatial variability. Our results demonstrate chronic and spatially extensive HAB toxins associated with elevated *chl-a,* but demonstrate a potential for HAB impacts rather than current impairments. The extent to which HAB toxins in SFB impair human and wildlife health from either chronic or acute exposure is unknown. In-depth investigations focusing on accu-mulation of toxins in higher trophic levels and the relationship between HAB sources and *chl-a* (e.g. ocean and riverine end-members as sources of cells and toxin) would strengthen the re-lationships identified in this analysis.

Second, processes underlying negative relationships between DO and *chl-a* are not well understood. We found a strong rela-tionship between summer DO and mean, seasonal *chl-a* from February–September, suggesting a link of biomass accumulation in spring to DO consumption in summer, as observed elsewhere (Hagy et al., 2004; Murphy et al., 2011). The accepted conceptual model for this relationship is a spatial and temporal displacement of phytoplankton biomass accumulation from microbial decomposi-tion and net ecosystem heterotrophy (Caffrey, 2003). This model may not adequately explain relationships of DO and *chl-a* as the largest increase of *chl-a* in SFB consisted of an elevated summer baseline from 1993 to 2014 (Fig. 4). Empirical relationships be-tween DO and *chl-a* presented here for SB and LSB will require further elucidation of phytoplankton contributions to the carbon budget and effects on benthic and pelagic respiration (e.g., Murrell et al., 2013).

We recognize that predictive relationships between HAB, DO and *chl-a* are inexact and are affected by fundamental drivers of phytoplankton dynamics that can be altered by climate and other factors. Therefore, the *chl*-a thresholds presented here should be considered as a starting place and should be re-evaluated regularly. SFB is a highly dynamic estuary that will continue to change throughout the next century (Cloern et al., 2011). The *chl-a* thresholds based on the analyses presented here relate to current endpoints and provide useful reference points for nutrient man-agement (Sutula and Senn, 2017). Uncertainties about ecological risks evident in relationships of HAB and DO to *chl-a* suggest that thresholds be applied as one of several lines of evidence to avoid water-quality degradation. Other lines of evidence could include direct measurements of ecological end-points (i.e., HAB cell den-sities and toxins, DO). We recommend that these *chl-a* thresholds guide testable hypotheses in ongoing monitoring and numerical modeling of SFB to refine risk assessments and explore causal mechanisms.

5. Summary

- Overt symptoms of anthropogenic eutrophication have not been expressed to date in SFB, as DO is higher and *chl-a* lower than in estuaries experiencing nutrient over-enrichment.
- Several recent trends suggest the potential for degradation of this ecosystem, including ubiquitous HAB, decreasing DO, and increasing *chl-a*. For example, HAB abundance exceeded alert levels in ~35% of samples over the last 20 years.
- Regression analyses revealed significant relationships of HAB abundance to *chl-a,* and of DO to *chl-a*, supporting a conceptual model linking increased risks of HAB and low DO to increased phytoplankton biomass.

- Thresholds for *chl-a* based on HAB and DO impairment converged on similar values. Monthly *chl-a* of 13 mg m^{-3} was an inflection point for reduced probability of exceeding alert levels for HAB abundance and toxins. This threshold was similar to 13–16 mg m^{-3} associated with attainment of the WQC for DO. At the opposite end of the risk continuum, *chl-a* thresholds representing a high probability of exceeding HAB alerts were within the same range of seasonal mean *chl-a* thresholds in which LSB and SB could fail to meet DO WQC of 5.0 mg L^{-1} (25–40 mg m^{-3}).
- *Chl-a* thresholds derived from quantitative analysis linked to risks of impairment can serve as guidance for managers to protect SFB from eutrophication problems that have severely affected estuaries around the world.
- The novel approach to deriving *chl-a* thresholds developed here is transferable to other estuaries to protect against eutrophication.

Appendix A. Supplementary data

Supplementary data related to this article can be found at http://dx.doi.org/10.1016/j.ecss.2017.07.009.

References

Andersen, J.H., Murray, C., Kaartokallio, H., Axe, P., Molvær, J., 2010. Confidence rating of eutrophication status classification. Mar. Pollut. Bull. 60, 919–924.

Andersen, J.H., Carstensen, J., Conley, D.J., Dromph, K., Fleming-Lehtinen, V., Gustafsson, B.G., Josefson, A.B., Norkko, A., Villnas, A., Murray, C., 2015. Long-term temporal and spatial trends in eutrophication status of the Baltic Sea. Biol. Rev. http://dx.doi.org/10.1111/brv.12221.

Bailey, H., Curran, C., Poucher, S., Sutula, M., 2014. Science supporting dissolved oxygen objectives for Suisun Marsh. Southern California Coastal Water Research Project Authority Technical Report 830. www.sccwrp.org, 33 pp.

Barber, R.T., Hiscock, M.R., 2006. A rising tide lifts all phytoplankton: growth response of other phytoplankton taxa in diatom-dominated blooms. Global Biogeochem. Cycles 20, GB4S03,. http://dx.doi.org/10.1029/2006GB002726.

Bricker, S.B., Ferreira, J.G., Simas, T., 2003. An integrated methodology for assess-ment of estuarine trophic status. Ecol. Modell. 169, 39–60.

Bricker, S., Longstaff, B., Dennison, W., Jones, A., Boicourt, C., Wicks, C., Woerner, J., 2007. Effects of Nutrient Enrichment in the Nation's Estuaries: a Decade of Change. NOAA Coastal Ocean Program Decision Analysis Series No. 26. National Centers for Coastal Ocean Science, Silver Spring, Maryland, USA, 328 pp.

Cade, B.S., Noon, B.R., 2003. A gentle introduction to quantile regression for ecol-ogists. Front. Ecol. Environ. 1, 412–420.

Caffrey, J.M., 2003. Production, respiration and net ecosystem metabolism in US estuaries. Environ. Mon. Assess. 81, 207–219.

Campbell, J.W., 1995. The lognormal distribution as a model for bio-optical vari-ability in the sea. J. Geophys. Res. 100, 13237–13254.

Cloern, J.E., 1982. Does the benthos control phytoplankton biomass in South San Francisco bay (USA)? Mar. Ecol. Progr. Ser. 9, 191–202.

Cloern, J.E., 2001. Our evolving conceptual model of the coastal eutrophication problem. Mar. Ecol. Prog. Ser. 210, 223–253.

Cloern, J.E., Dufford, R., 2005. Phytoplankton community ecology: principles applied in San Francisco Bay. Mar. Ecol. Prog. Ser 285, 11–28.

Cloern, J.E., Jassby, A., 2008. Complex seasonal patterns of primary producers at the land-sea interface. Ecol. Lett. 11, 1294–1303. http://dx.doi.org/10.1111/j.1461-0248.2008.01244.

Cloern, J.E., Jassby, A.D., 2012. Drivers of change in estuarine-coastal ecosystems: discoveries from four decades of study in San Francisco Bay. Rev. Geophys 50, RG4001. http://dx.doi.org/10.1029/2012RG000397.

Cloern, J.E., Schraga, T.S., 2016. USGS Measurements of Water Quality in San Fran-cisco Bay (CA), 1969-2015: U. S. Geological Survey data release. https://doi.org/10.5066/F7TQ5ZPR.

Cloern, J.E., Cole, B.E., Hager, S.W., 1994. Notes on *Mesodinium rubrum* red tides in San Francisco bay (California, USA). J. Plankton Res. 16, 1269–1276.

Cloern, J.E., Schraga, T.S., Lopez, C.B., Knowles, N., Labiosa, R.G., Dugdale, R., 2005.

Climate anomalies generate an exceptional dinoflagellate bloom in San Francisco Bay. Geophys. Res. Lett. 32, L14608. http://dx.doi.org/10.1029/2005GL023321.

Cloern, J., Jassby, A., Thompson, J., Hieb, K., 2007. A cold phase of the East Pacific triggers new phytoplankton blooms in San Francisco Bay. Proc. Natl. Acad. Sci. U. S. A. 104, 18,561–18,565.

Cloern, J.E., Knowles, N., Brown, L.R., Cayan, D., Dettinger, M.D., Morgan, T.L., Schoellhamer, D.H., Stacey, M.T., van der Wegen, M., Wagner, R.W., Jassby, A., 2011. Projected evolution of California's San Francisco Bay-Delta-River System in a century of climate change. PLoS One 6, e24465. http://dx.doi.org/10.1371/journal.pone.0024465.

Cloern, J.E., Abreu, P.C., Carstensen, J., Chauvaud, L., Elmgren, R., Grall, J., Greening, H., Johansson, J.O.R., Kahru, M., Sherwood, E.T., Xu, J., Yin, K., 2015. Human activities and climate variability drive fast-paced change across the world's estuarine-coastal ecosystems. Glob. Chang. Biol. http://dx.doi.org/10.1111/gcb.13059.

Devlin, M., Bricker, S., Painting, S., 2011. Comparison of five methods for assessing impacts of nutrient enrichment using estuarine case studies. Biogeochemistry 106, 177–205.

Diaz, R.J., Rosenberg, R., 1995. Marine benthic hypoxia: a review of its ecological effects and the behavioral responses of benthic macrofauna. Oceanogr. Mar. Biol. Ann. Rev. 33, 245–303.

Diaz, R.J., Rosenberg, R., 2008. Spreading dead zones and consequences for marine ecosystems. Science 321, 926–929.

Duarte, C.M., Conley, D.J., Carstensen, J., Sánchez-Camacho, M., 2009. Return to Neverland: shifting baselines affect eutrophication restoration targets. Estuar. Coasts 32, 29–36.

Gibble, C., Kudela, R., 2014. Detection of persistent microcystins toxins at the land-sea interface in Monterey Bay, California. Harmful Algae 39, 146–153. http://dx.doi.org/10.1016/j.hal.2014.07.004.

Glibert, P.M., Anderson, D.M., Gentien, P., Graneli, E., Sellner, K.G., 2005. The global, complex phenomena of harmful algal blooms. Oceanography 18, 137–147.

Goldstein, T., Mazet, J.A.K., Zabka, T.S., Langlois, G., Colegrove, K.M., Silver, M., Bargu, S., Van Dolah, F., Leighfield, T., Conrad, P.A., Barakos, J., Williams, D.C., Dennison, S., Haulena, M., Gulland, F.M.D., 2008. Novel symptomatology and changing epidemiology of domoic acid toxicosis in California sea lions Zalophus californianus: an increasing risk to marine mammal health. Proc. R. Soc. B Biol. Sci. 275, 267–276.

Hagy, J.D., Boynton, W.R., Keefe, C.W., Wood, K.V., 2004. Hypoxia in Chesapeake Bay, 1950–2001: Long-term Change in Relation to Nutrient Loading and River Flow. Estuaries 27, 634–658.

Harding Jr., L.W., Batiuk, R.A., Fisher, T.R., Gallegos, C.L., Malone, T.C., Miller, W.D., Mulholland, M.R., Paerl, H.W., Perry, E.S., Tango, P., 2014. Scientific bases for numerical chl-a criteria in Chesapeake Bay. Estuar. Coasts 37, 134–148.

Harding Jr., L.W., Gallegos, C.L., Perry, E.S., Miller, W.D., Adolf, J.E., Mallonee, M.E., Paerl, H.W., 2015. Long-term trends of nutrients and phytoplankton in Chesapeake Bay. Estuar. Coasts. http://dx.doi.org/10.1007/sl2237-015-0023-7.

Harding Jr., L.W., Mallonee, M.E., Perry, E.S., Miller, W.D., Adolf, J.E., Gallegos, C.L., Paerl, H.W., 2016. Variable Climatic Conditions Dominate Recent Phytoplankton Dynamics in Chesapeake Bay. http://dx.doi.org/10.1038/srep23773. http://nature.com/scientificreports/6:23773.

Heisler, J., Glibert, P.M., Burkholder, J.M., Anderson, D.M., Cochlan, W., Dennison, W.C., Dortch, Q., Gobler, C.H., Heil, C.A., Humphries, E., Lewitus, A., Magnien, R., Marshall, H.G., Sellner, K.G., Stockwell, D.A., Suddleson, M., 2008. Eutrophication and harmful algal blooms: a scientific consensus. Harmful Algae 8, 3–13.

Hollister, J., Walker, H., Paul, J.F., 2008. CProb: a computational tool for conducting conditional probability analysis. J. Environ. Qual. 37, 2392–2396.

Jassby, A.D., Cole, B.E., Cloern, J.E., 1997. The design of sampling transects for characterizing water quality in estuaries. Estuar. Coast. Shelf Sci. 45, 285–302.

Kemp, W.M., Boynton, W.R., Adolf, J.E., Boesch, D.F., Boicourt, W.C., Brush, G., Cornwell, J.C., Fisher, T.R., Glibert, P.M., Hagy, J.D., Harding Jr., L.W., Houde, E.D., Kimmel, D.G., Miller, W.D., Newell, R.I.E., Roman, M.R., Smith, E.M., Stevenson, J.C., 2005. Eutrophication of Chesapeake Bay: historical trends and ecological interactions. Mar. Ecol. Progr. Ser. 303, 1–29.

Kudela, R.M., 2011. Characterization and deployment of Solid Phase Adsorption Toxin Tracking (SPATT) resin for monitoring of microcystins in fresh and saltwater. Harmful Algae 11, 117–125.

Lane, J.Q., Roddam, C.M., Langlois, G.W., Kudela, R.M., 2010. Application of Solid Phase Adsorption Toxin Tracking (SPATT) for field detection of domoic acid and saxitoxin in coastal California. Limnol. Oceanogr. Methods 8, 645–660.

Lehman, P.W., Boyer, G., Hall, C., Waller, S., Gehrts, K., 2005. Distribution and toxicity of a new colonial Microcystis aeruginosa bloom in the San Francisco bay estuary, California. Hydrobiol 541, 87–99.

Lehman, P.W., Teh, S.J., Boyer, G.L., Nobriga, M., Bass, E., Hogle, C., 2010. Initial impacts of Microcystis on the aquatic food web in the San Francisco estuary. Hydrobiol 637, 229–248.

Lewitus, A.J., Horner, R.A., Caron, D.A., Garcia-Mendoza, E., Hickey, B.M., Hunter, M., Huppert, D.D., Kudela, R.M., Langlois, G.W., Largier, J.L., 2012. Harmful algal blooms along the North American west coast region: history, trends, causes, and impacts. Harmful Algae 19, 133–159.

Lundholm, N., Moestrop, O., 2006. The biogeography of harmful algae. In:

Granelli, E., Turner, J.T. (Eds.), Ecology of Harmful Algae, vol. 189. Springer. Ecological Studies.

Mackenzie, L., Beuzenberg, V., Holland, P., Mcnabb, P., Selwood, A., 2004. Solid phase adsorption toxin tracking (SPATT): a new monitoring tool that simulates the biotoxin contamination of filter feeding bivalves. Toxicon 44, 901–918. http://dx.doi.org/10.1016/j.toxicon.2004.08.020.

McCabe, R.M., Hickey, B.M., Kudela, R.M., Lefebvre, K.A., Adams, N.G., Bill, B.D., Gulland, F.M.D., Thomson, R.E., Cochlan, W.P., Trainer, V.L., 2016. An Unprecedented Coastwide Toxic Algal Bloom Linked to Anomalous Ocean Conditions. Submitted.

Montie, E.W., Wheeler, E., Pussini, N., Battey, T.W.K., Van Bonn, W., Gulland, F., 2012. Magnetic resonance imaging reveals that brain atrophy is more severe in older California sea lions with domoic acid toxicosis. Harmful Algae 20, 19–29.

Murphy, R.R., Kemp, W.M., Ball, W.P., 2011. Long-term trends in Chesapeake Bay seasonal hypoxia, stratification, and nutrient loading. Estuar. Coasts 34, 1293–1309.

Murrell, M.C., Stanley, R., Lehrter, J.C., Hagy, J.D., 2013. Plankton community respiration, net ecosystem metabolism, and oxygen dynamics on the Louisiana continental shelf: implications for hypoxia. Cont. Shelf Res. 52, 27–37.

National Research Council, 2009. Science and Decisions: Advancing Risk Assessment. Committee on Improving Risk Analysis Approaches Used by U.S. EPA. Board on Environmental Studies and Toxicology. http://dx.doi.org/10.17226/12209.

Nixon, S.W., 1995. Coastal marine eutrophication: a definition, social causes, and future concerns. Ophelia 41, 199–219.

Paerl, H.W., 1997. Coastal eutrophication and harmful algal blooms: importance of atmospheric deposition and groundwater as "new" nitrogen and other nutrient sources. Limnol. Oceanogr. 42, 1154–1165.

Paul, J.F., McDonald, M.E., 2005. Development of empirical, geographically-specific water quality criteria: a conditional probability analysis approach. J. Am. Water Resour. Assoc. 41, 1211–1223.

Rabalais, N.N., Cai, W.-J., Carstensen, J., Conley, D.J., Fry, B., Hu, X., Quiñones-Rivera, z., Rosenberg, R., Slomp, C.P., Turner, R.E., Voss, M., Wissel, B., Zhang, J., 2014. Eutrophication-driven deoxygenation in the coastal ocean. Oceanography 27, 172–183.

Raimonet, M., Cloern, J.E., 2017. Estuary–ocean connectivity: fast physics, slow biology. Glob. Change Biol. 23, 2345–2357. http://dx.doi:10.1111/gcb.13546.

Riemann, B., Carstensen, J., Dahl, K., Fossing, H., Hansen, J.W., Jakobsen, H.H., Josefson, A.A., Krause-Jensen, D., Markager, S., Stæhr, P.A., Timmermann, K., Windolf, J., Andersen, J.H., 2015. Recovery of Danish coastal ecosystems after reductions in nutrient loading: a holistic ecosystem approach. Estuar. Coasts. http://dx.doi.org/10.1007/s12237-015-9980-0.

Rosenberg, R., Hellman, B., Johansson, B., 1991. Hypoxic tolerance of marine benthic fauna. Mar. Ecol. Prog. Ser. 79, 127–131.

San Francisco Bay Regional Water Quality Control Board (SFRWQCB), 2015. San Francisco Bay Basin (Region 2) Water Quality Control Plan. As amended March 2015, available at: www.waterboards.ca.gov/rwqcb2/basin_planning.shtml.

Schaeffer, B.A., Hagy, J.D., Conmy, R.N., Lehrter, J.C., Stumpf, R.P., 2012. An approach to developing numeric water quality criteria for coastal waters using the SeaWiFS satellite data record. Environ. Sci. Technol. 46, 916–922.

Shellenbarger, G.G., Schoellhamer, D.H., Morgan, T.L., Takekawa, J.Y., Athearn, N.D., Henderson, K.D., 2008. Dissolved Oxygen in Guadalupe Slough and Pond A3W, South San Francisco Bay, California, August and September 2007. U.S. Geological Survey Open-File Report 2008–1097, 26 pp.

Shutler, J.D., Davidson, K., Miller, P.I., Swan, S.C., Grant, M.G., Bresnan, E., 2012. An adaptive approach to detect high-biomass algal blooms from EO chl-a-a data in support of harmful algal bloom monitoring. Rem. Sens. Lett. 3, 101–110.

Silke, J., O'Beirn, F., Cronin, M., 2005. Karenia: an exceptional dinoflagellate bloom in western Irish waters, summer 2005. Mar. Environ. Health Ser. 21, 44 pp.

Smith, S.V., Hollibaugh, J.T., 2006. Water, salt, and nutrient exchanges in San Francisco bay. Limnol. Oceanogr. 51, 504–517.

Sutula, M., Senn, D., 2017. Scientific Bases for Assessment of Nutrient Impacts on San Francisco Bay. Southern California Coastal Water Research Project Authority Technical Report 864. www.sccwrp.org, 56 pp.

Thébault, J., Schraga, T.S., Cloern, J.E., Dunlavey, E.G., 2008. Primary production and carrying capacity of former salt ponds after reconnection to San Francisco Bay. Wetlands 28, 841–851.

U.S. Environmental Protection Agency, 1998. Guidelines for Ecological Risk Assessment. EPA/630/R-95/002F.

Vlamis, A., Katikou, P., 2014. Climate influence on Dinophysis spp. spatial and temporal distributions in Greek coastal water. Plankton Benthos Res. 9, 15–31.

Wheeler, P.A., Huyer, A., Fleischbein, J., 2003. Cold halocline, increased nutrients and higher chl-a off Oregon in 2002. Geophys. Res. Lett. 30 http://dx.doi.org/10.1029/2003GL017395.

White, A.E., Watkins-Brandt, K.S., McKibben, S.M., Wood, A.M., Hunter, M., Forster, Z., Du, X., Peterson, W.T., 2014. Large-scale bloom of Akashiwo sanguinea in the Northern California current system in 2009. Harmful Algae 37, 38–46.

WHO, 2003. Coastal and fresh waters. Guidelines for Safe Recreational Water Environments, vol. 1. World Health Organization, Geneva, Switzerland, 219 pp.

Zaldivar, J.M., Viaroli, P., Newton, A., De Wit, R., Ibanez, C., Reizopoulou, S., Somma, F., Razinkovas, A., Basset, A., Holmer, M., Murray, N., 2008. Eutrophication in transitional waters: an overview. Trans. Waters Monogr. 1, 1–78.